Mechanics Of Soft Materials
https://doi.org/10.1007/s42558-019-0008-y

ORIGINAL PAPER

Constitutive model of human artery adventitia enhanced with a failure description

K. Y. Volokh[1]

Received: 15 October 2018 / Accepted: 15 April 2019

Abstract
A constitutive model of a human artery adventitia is presented and calibrated in uniaxial tension tests in longitudinal and circumferential directions. Both the experiment and the model describe the descending branch of the stress-stretch curve and, thus, failure becomes a part of the constitutive law. The theoretical failure description is provided by the introduction of energy limiters and it does not use internal damage variables. The latter feature allows for an easy analysis of material instability and the onset of failure. Particularly, the failure envelope is created in biaxial tension under various stretch ratios. In addition, the loss of ellipticity is analyzed in equibiaxial stretch and pure shear and it is found that the localized failure—crack—is approximately aligned with the directions of collagen fibers in accordance with experimental observations.

Keywords Human artery adventitia · Energy limiters · Stress-stretch curve

1 Introduction

Adventitia is the external layer of the arterial wall which plays the crucial role in sustaining mechanical integrity of the artery under extreme conditions: aneurysm development, balloon angioplasty, supraphysiological loads, etc. Under extreme conditions, the adventitia may rupture threatening health and life [13]. It is essential, thus, to comprehend mechanical properties of the adventitia including its stiffness and, especially, strength. Modeling and in vitro testing can improve our understanding of the adventitia mechanical behavior in vivo.

In contrast to other arterial layers—intima and media—adventitia is strong mechanically due to the sound presence of bundles of collagen fibers embedded in soft ground matrix. When straightened, the wavy collagen fibers contribute significantly to stiffness and strength of the adventitia. From the mechanics standpoint, the adventitia layer, as well as the media, is a fiber-reinforced soft composite material. The constitutive modeling of such an arterial wall material has a three-decade history including, for example, the works by [3, 7–9, 11, 12, 14, 15, 27, 34] and many others recently reviewed by [10]. It is not surprising, of course, that most studies were focused on a description of the intact mechanical behavior. Incorporation of a failure description in the constitutive theories has begun relatively recently including, for example, the works by [2, 4, 6, 17, 18, 20–22, 25, 26] and others reviewed by [16].

Mentioned works on modeling tissue failure usually introduce a damage variable to reduce material stiffness. The damage variable is defined by an evolution law when it obeys the damage threshold condition. The damage variable is not easy to interpret in physically appealing terms and it is essentially the so-called internal variable. Despite the interpretation difficulties, the damage variable is instrumental when a gradual and incomplete material failure develops (e.g., Mullins effect). If the failure is complete and abrupt, much simpler approach of energy limiters, e.g., [1, 29, 30], can be used without introduction of internal variables. Energy limiters enforce saturation value for the strain energy, the failure energy, which

✉ K. Y. Volokh
cvolokh@technion.ac.il

[1] Faculty of Civil and Environmental Engineering, Technion - Israel Institute of Technology, Haifa, Israel

Published online: 03 May 2019

automatically bounds stresses in the constitutive equations. Physically, the failure energy is an average energy of molecular bonds.

In the present work, we develop a novel constitutive model of a human adventitia based on the uniaxial tension tests in the longitudinal (axial) and circumferential directions of an artery (Section 2). This constitutive model is essentially the Holzapfel-Gasser-Ogden theory [9] enhanced with the energy limiters. The calibration of the theory is performed for the adventitia sample in uniaxial tension (Section 3). The use of the energy limiters in the constitutive model allows us to easily analyze instability of the adventitia sheet in biaxial tension and create the failure envelope (Section 4). Moreover, the developed constitutive theory allows to analyze the loss of ellipticity and predict the preferable directions of failure localization into cracks (Section 5).

2 Constitutive theory: HGO model with energy limiters

In this section, we generalize the HGO [9] model by inserting the energy limiters in it. For the general background on the elasticity with energy limiters, the work by [31–33] might be useful.

We use the continuum mechanics approach according to which the discrete molecular composition of materials is approximated by a continuously distributed set of the so-called material points. We designate position of a generic material point in the initial configuration Ω_0 by $\mathbf{x}$ and its position in the current configuration Ω by $\mathbf{y}(\mathbf{x})$. The deformation gradient is $\mathbf{F} = \text{Grad}\mathbf{y}$. We also assume that material is incompressible and, consequently, $J = \det\mathbf{F} = 1$.

We define the strain energy function for adventitia per unit reference volume as a sum of three terms

$$\psi = \psi_1 + \psi_4 + \psi_6. \tag{1}$$

Here, ψ_1 is the strain energy of the ground matrix

$$\psi_1 = \frac{c}{2}(I_1 - 3)H(\zeta_4)H(\zeta_6) \tag{2}$$

where $H(\zeta_i)$ is a step function, i.e., $H(\zeta_i) = 0$ if $\zeta_i < 0$ and $H(\zeta_i) = 1$; otherwise, c is a material constant; and the first principal invariant is defined as follows

$$I_1 = \mathbf{F} : \mathbf{F} = F_{ij}F_{ij}, \tag{3}$$

where the sum over the repeated indices is implied.

The strain energies of two families of collagen fibers are

$$\begin{aligned}\psi_4 &= H(\zeta_6)\{\psi_4^{\text{f}} - H(\zeta_4)\psi_4^{\text{e}}\},\\ \psi_6 &= H(\zeta_4)\{\psi_6^{\text{f}} - H(\zeta_6)\psi_6^{\text{e}}\}.\end{aligned} \tag{4}$$

Here, ψ_i^{f} and ψ_i^{e} are the failure and elastic energies of the collagen fibers in the form

$$\psi_i^{\text{f}} = \Phi_i m_i^{-1}\Gamma(m_i^{-1}, 0), \quad \psi_i^{\text{e}} = \Phi_i m_i^{-1}\Gamma(m_i^{-1}, W_i^{m_i}\Phi_i^{-m_i}), \quad i = 4, 6, \tag{5}$$

where $\Gamma(s, x) = \int_x^\infty a^{s-1}e^{-a}da$ is the upper incomplete gamma function and Φ_i, m_i are material failure constants.

We note that the energy limiter Φ_i physically means the average bond energy (see [28] for further details).

The strain energy of the intact collagen fibers follows [9]

$$W_i = \frac{k_1}{2k_2}\{\exp[k_2(I_i - 1)^2] - 1\}, \quad i = 4, 6, \tag{6}$$

where k_1, k_2 are material parameters and invariants I_4 and I_6 represent squared fiber length after the deformation

$$I_4 = |\mathbf{F}\mathbf{m}_0|^2, \quad I_6 = \left|\mathbf{F}\mathbf{m}_0'\right|^2, \tag{7}$$

where

$$[\mathbf{m}_0] = [0, \sin\beta, \cos\beta]^{\text{T}}, \quad [\mathbf{m}_0'] = [0, -\sin\beta, \cos\beta]^{\text{T}} \tag{8}$$

designate components of unit vectors in the directions of two fiber families (Fig. 1).

The two fiber families are symmetric and inclined with angle $\pm\beta$ with respect to the longitudinal direction of the artery.

It is important to emphasize that the fibers are active and contribute to the strain energy in tension only

$$I_4 > 1, \quad I_6 > 1. \tag{9}$$

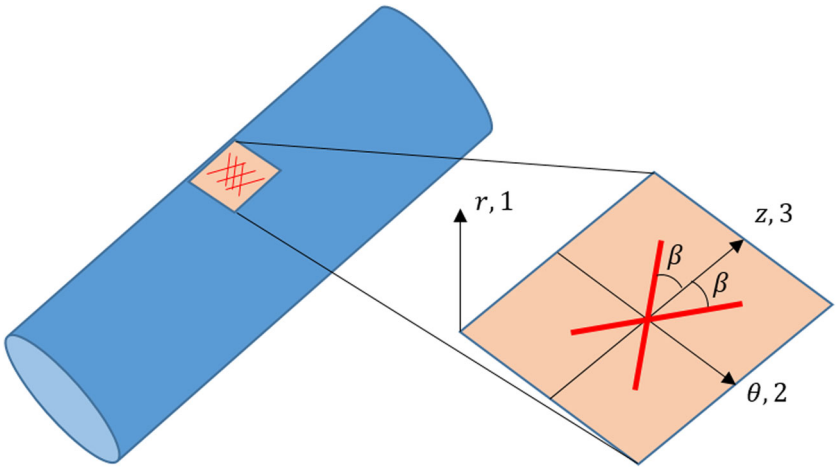

Fig. 1 Radial (1 or r), circumferential (2 or θ), and longitudinal (3 or z) directions in the artery

We note that the switch parameter $\zeta_i \in (-\infty, 0]$ is defined by the evolution equation

$$\dot{\zeta}_i = -H(\epsilon_i - \psi_i^{\mathrm{e}}/\psi_i^{\mathrm{f}}), \quad \zeta_i(t=0) = 0, \quad i = 4, 6, \tag{10}$$

where $0 < \epsilon_i \ll 1$ is a dimensionless precision constant.

The proposed constitutive law can be interpreted as follows. The material response is hyperelastic before the strain energy reaches its limit ψ_i^{f}. After that, the strain energy remains constant and equal ψ_i^{f} preventing from the material healing and providing the energy dissipation. Parameter ζ_i is not an internal variable describing damage—it is rather a switch: if $\zeta_i = 0$, then the process is elastic and if $\zeta_i < 0$, then the material is irreversibly damaged and the strain energy is dissipated. The present setting presumes (via step function multipliers) that the failure of any family of fibers leads to the automatic failure of the whole adventitia layer. We should note that the irreversibility and dissipation issue is important in the case of unloading. If only loading is considered, like in the present work, then it is possible to set

$$\zeta_4 = \zeta_6 = 0 \Rightarrow H(\zeta_4) = H(\zeta_6) = 1. \tag{11}$$

3 Uniaxial tension: calibration

When a thin strip of the adventitia sample is stretched in its plane in the directions of the symmetry axes, that is longitudinal and circumferential arterial directions, then these directions are the principal ones and the constitutive equations can be written as follows [24]

$$\sigma_r = 0, \quad \sigma_\theta = \lambda_\theta \frac{\partial \hat{\psi}}{\partial \lambda_\theta}, \quad \sigma_z = \lambda_z \frac{\partial \hat{\psi}}{\partial \lambda_z}, \tag{12}$$

where

$$\hat{\psi}(\lambda_\theta, \lambda_z) = \psi(\lambda_\theta^{-1}\lambda_z^{-1}, \lambda_\theta, \lambda_z). \tag{13}$$

We use the subscripts of the cylindrical system of coordinates related to the arterial wall globally for the purpose of the plane stress analysis. The latter means that characters r, θ, z can be replaced by numbers 1, 2, 3 accordingly (see Fig. 1).

In the case of isotropy, only one of three stretches is independent and the uniaxial tension simulation is trivial. In the case of anisotropy under consideration, both stretches, λ_θ and λ_z, are independent and simultaneous solution of Eq. $12_{2\text{-}3}$ is required. In the case of stretching in longitudinal z-direction, the coupled system

$$\frac{\partial \hat{\psi}}{\partial \lambda_\theta} = 0, \quad \sigma_z = \lambda_z \frac{\partial \hat{\psi}}{\partial \lambda_z}$$

is solved, while in the case of stretching in circumferential θ-direction, the coupled system

$$\sigma_\theta = \lambda_\theta \frac{\partial \hat{\psi}}{\partial \lambda_\theta}, \quad \frac{\partial \hat{\psi}}{\partial \lambda_z} = 0$$

is solved.

Table 1 Model calibration

c (KPa)	k_1 (KPa)	k_2	β°	$\Phi_4 = \Phi_6$ (KPa)	$m_4 = m_6$
75	1500	0.03	45.8	95	1.2

The process of the parameter fitting is by no means trivial and it requires both the insight into the role of the model parameters and the least squares minimization procedure.[1] The fitting results are presented in Table 1.

Stress-stretch diagrams for the calibrated model are shown on the left of Figs. 2 and 3.

The experimental data including the descending parts of the stress-stretch curves was obtained in the uniaxial tension tests for the coronary tissue performed in the Institute of Biomechanics at the Graz University of Technology (see also the "Acknowledgments" section).

4 Failure envelope

The developed constitutive model of adventitia incorporating a failure description via energy limiters allows us to create the failure envelope. We assume that a thin adventitia layer is in biaxial tension with the varying ratios of the longitudinal and circumferential stretches. The stress-stretch state is homogeneous and it becomes critical when the determinant of the Hessian of the strain energy vanishes

$$H(\lambda_\theta, \lambda_z) = \det \begin{bmatrix} \partial^2\hat{\psi}/\partial\lambda_\theta^2 & \partial^2\hat{\psi}/\partial\lambda_\theta\partial\lambda_z \\ \partial^2\hat{\psi}/\partial\lambda_\theta\partial\lambda_z & \partial^2\hat{\psi}/\partial\lambda_z^2 \end{bmatrix} = 0. \tag{14}$$

Equation 14 defines a curve—failure envelope—in the space of stretches that can be generated numerically (see Fig. 4).

The envelope comes from the constitutive equations and it is a good replacement for the intuitive strength-of-materials local failure criteria often used in various branches of engineering. It is worth noting that the critical stretches in the case of equibiaxial stretching are less than in the case of uniaxial tension. The latter observation means that the traditional definition of the material strength as a critical stress in uniaxial experiments is not applicable to other states of deformation. Moreover, the use of the "uniaxial strength" can be dangerous because failure can occur before this strength is reached as it is readily seen from Fig. 4.

5 Loss of ellipticity and crack direction

Further studies on the onset of failure can be done by analysis of the propagation of plane waves superimposed on the deformed state of material (see [23] or [33] for the general background). Particularly, a plane wave is prescribed in the form

$$\tilde{\mathbf{y}}(\mathbf{y}) = \mathbf{r}g(\mathbf{s}\cdot\mathbf{y} - wt), \tag{15}$$

where unit vectors $\mathbf{r}$ and $\mathbf{s}$ give the directions of the wave polarization and propagation accordingly; g is a twice differentiable function; and w is the wave speed.

Importantly, in the case of the incompressible material, the directions of wave polarization and propagation are mutually orthogonal

$$\mathbf{r}\cdot\mathbf{s} = 0. \tag{16}$$

Substitution of the plane wave solution in the incremental equations of the initial boundary-value problem of nonlinear elasticity, which we omit here for the sake of brevity, gives the mass density (ρ)-weighted squared wave speed in the form

$$\rho w^2 = \mathbf{r}\cdot\mathbf{\Lambda}(\mathbf{s})\mathbf{r}, \tag{17}$$

where

$$\Lambda_{ik} = A_{ijkl}s_j s_l \tag{18}$$

[1] Particularly, the initial guess is crucial and not obvious.

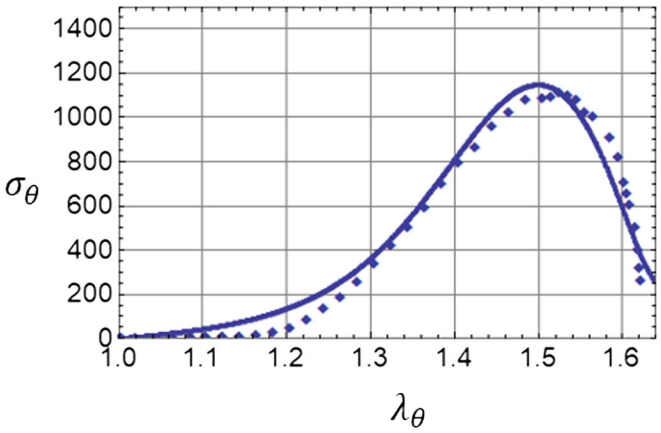

Fig. 2 Circumferential Cauchy stress (KPa) versus circumferential stretch: solid lines for the theory and squares for the experimental data

is the second-order acoustic tensor and

$$A_{ijkl} = F_{js} F_{lm} \frac{\partial^2 \psi}{\partial F_{is} \partial F_{km}} \tag{19}$$

is the fourth-order elasticity tensor.

Intact material can propagate waves and, consequently,

$$\rho w^2 > 0. \tag{20}$$

If material failed, then it cannot propagate elastic waves anymore and

$$\rho w^2 = 0, \tag{21}$$

which is also called the condition of the loss of ellipticity (see [23] for the terminology motivation).

Thus, condition (21) can be used to find the failing wave. Remember that due to the incompressibility constraint, the vector of the wave polarization is perpendicular to the wave direction and it can be interpreted as the direction of failure localization. In other words, **r** can be interpreted as the direction of the crack when condition (21) is obeyed.

In the case of plane stress under consideration, we specify the wave vectors as follows

$$[\mathbf{s}] = [0, \sin\alpha, \cos\alpha]^{\mathrm{T}}, \quad [\mathbf{r}] = [0, \cos\alpha, -\sin\alpha]^{\mathrm{T}}. \tag{22}$$

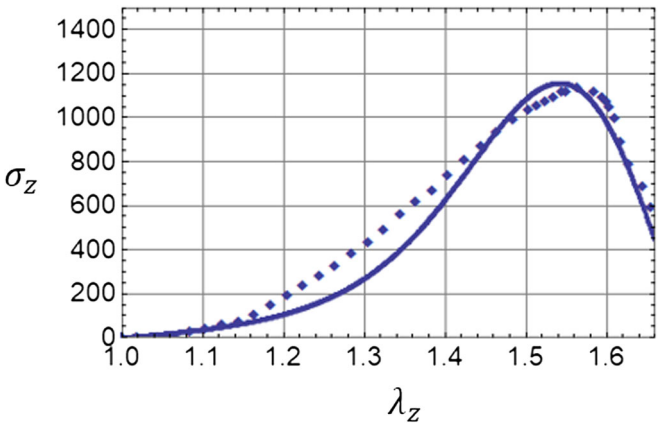

Fig. 3 Longitudinal Cauchy stress (KPa) versus longitudinal stretch: solid lines for the theory and squares for the experimental data

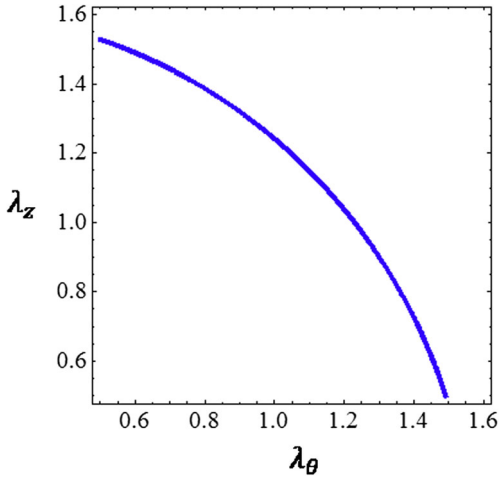

Fig. 4 Failure envelope: the curve presents critical stretches where the determinant of the Hessian vanishes according to (14)

Also, in the case of the given strain energy depending on three invariants $\psi(I_1, I_4, I_6)$, we calculate the elasticity tensor (omitting lengthy manipulations) as follows

$$\begin{aligned} A_{ijkl} = {} & 2\delta_{ik}\left(\frac{\partial\psi}{\partial I_1}B_{jl} + \frac{\partial\psi}{\partial I_4}m_j m_l + \frac{\partial\psi}{\partial I_6}m'_j m'_l\right) \\ & + 4\frac{\partial^2\psi}{\partial I_1^2}B_{ij}B_{kl} + 4\frac{\partial^2\psi}{\partial I_4^2}m_i m_j m_k m_l + 4\frac{\partial^2\psi}{\partial I_6^2}m'_i m'_j m'_k m'_l \\ & + 4\frac{\partial^2\psi}{\partial I_1\partial I_4}(B_{ij}m_k m_l + m_i m_j B_{kl}) \\ & + 4\frac{\partial^2\psi}{\partial I_1\partial I_6}(B_{ij}m'_k m'_l + m'_i m'_j B_{kl}) \\ & + 4\frac{\partial^2\psi}{\partial I_4\partial I_6}(m_i m_j m'_k m'_l + m'_i m'_j m_l m_k), \end{aligned} \tag{23}$$

where

$$\mathbf{B} = \mathbf{F}\mathbf{F}^{\mathrm{T}}, \quad \mathbf{m} = \mathbf{F}\mathbf{m}_0, \quad \mathbf{m}' = \mathbf{F}\mathbf{m}'_0. \tag{24}$$

It remains to choose the deformation states for analysis. In vivo, adventitia undergoes various states of biaxial stretching. We consider two limit cases. The first is the case of equibiaxial stretching in which

$$[\mathbf{F}] = \begin{bmatrix} \lambda^{-2} & 0 & 0 \\ 0 & \lambda & 0 \\ 0 & 0 & \lambda \end{bmatrix}. \tag{25}$$

Substitution of (22) and (25) in (21) yields condition

$$\rho w^2(\lambda, \alpha) = 0, \tag{26}$$

which defines a curve in the stretch-angle plane implicitly.

This numerically generated curve is shown in Fig. 5. It has minimum at $\alpha = 44^\circ$.

The second limit case is the case of pure shear (restrained tension) in the circumferential direction in which

$$[\mathbf{F}] = \begin{bmatrix} \lambda^{-1} & 0 & 0 \\ 0 & \lambda & 0 \\ 0 & 0 & 1 \end{bmatrix}. \tag{27}$$

Substitution of (22) and (27) in (21) yields the curve shown in Fig. 6. The minimum stretch is achieved for $\alpha = 40^\circ$.

In summary, the direction of localized failure or cracks (perpendicular to the wave directions) is very much aligned with the direction of fibers. On the other hand, this effect is based on the idealized material analyses which does not include material imperfections that can change the crack directions.

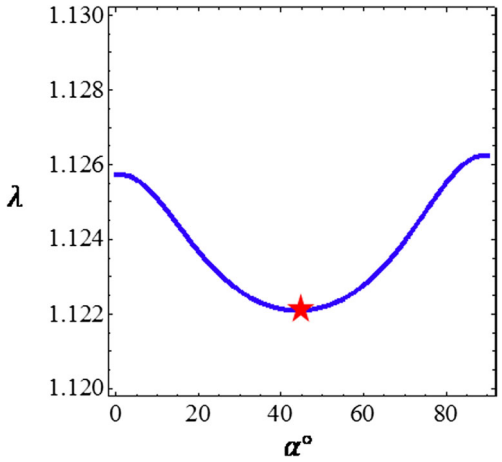

Fig. 5 Equibiaxial tension: $\rho w^2(\lambda, \alpha) = 0$ (star shows minimum)

6 Discussion

This work presents three novel results concerning mechanics of the human artery adventitia.

First, a new constitutive model is presented and calibrated in experiments. This model is a generalization of the Holzapfel-Gasser-Ogden (HGO) theory by incorporation of a failure description via energy limiters. The latter generalization is mathematically simple and physically appealing because it does not use internal variables. The introduced additional failure constants are calibrated in the macroscopic experiments. The developed model readily allows for analysis of the onset of failure. We note that the descending part of the stress-stretch curve is only a qualitative indicator of failure. Some more formal failure criteria are necessary. Specifically, we used the vanishing determinant of the Hessian and the loss of the strong ellipticity condition as the indicators of the onset of failure.

Second, the failure envelope is generated based on the developed constitutive model. The envelope comes from the constitutive equations and it is a good replacement for the intuitive strength-of-materials local failure criteria often used in various branches of engineering. Such simplified criteria can be misleading as in the case of the use of uniaxial tension strength for failure analysis in biaxial tension, for example.

Third, the loss of the strong ellipticity associated with the inability of the failed material to propagate superimposed waves is analyzed. It is found that the direction of localized failure or cracks is very much aligned with the direction of fibers. This finding is based on the idealized material analyses which does not include material imperfections that could change the crack directions. Nevertheless, this finding is in perfect correspondence with the very recent study by [19] who report that "the direction of the rupture (of thoracic aortic aneurysm) is aligned with the direction of maximum stiffness" which is

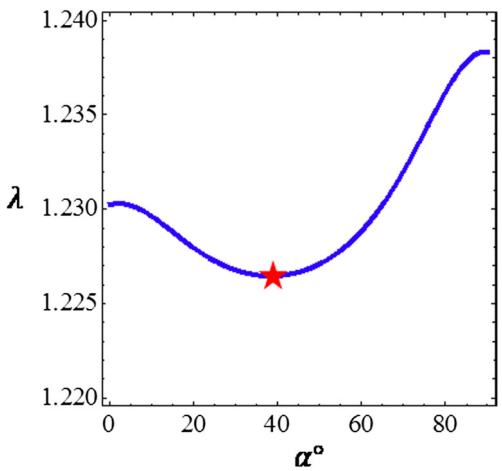

Fig. 6 Pure shear: $\rho w^2(\lambda, \alpha) = 0$ (star shows minimum)

the direction of fibers. It is also encouraging that [19] observe that "the rupture generally occurs at a location of the highest stored energy." The latter observation is in a good correspondence with the idea of considering limited strain energy as the basis for the constitutive model developed in the present work.

Finally, we should emphasize that only the onset of failure has been addressed in this work. The failure localization and development of cracks would require a regularized formulation as, for example, in [5].

Acknowledgments The author is grateful to Professor G.A. Holzapfel for providing the experimental data presented in Figs. 2 and 3.

Funding information This study is financially supported by the Israel Science Foundation (ISF 198/15).

Compliance with Ethical Standards

Conflict of interest The author declares that he has no conflict of interest.

References

1. Balakhovsky, K., Jabareen, M., Volokh, K.Y.: Modeling rupture of growing aneurysms. J. Biomech. **47**, 653–658 (2014)
2. Balzani, D., Brinkhues, S., Holzapfel, G.A.: Constitutive framework for the modeling of damage in collagenous soft tissues with application to arterial walls. Comp. Meth. Appl. Mech. Eng. **213**, 139–151 (2012)
3. Chuong, C.J., Fung, Y.C.: Three-dimensional stress distribution in arteries. J. Biomech. Eng. **105**, 268–274 (1983)
4. De Vita, R., Slaughter, W.S.: A constitutive law for the failure behavior of medial collateral ligaments. Biomech. Model Mechanobiol. **6**, 189–197 (2007)
5. Faye, A., Lev, Y., Volokh, K.Y.: The effect of local inertia around the crack tip in dynamic fracture of soft materials. Mech. Soft. Mater. **1**, 4 (2019)
6. Gasser, T.C.: An irreversible constitutive model for fibrous soft biological tissue: a 3-D microfiber approach with demonstrative application to abdominal aortic aneurysms. Acta. Biomater **7**, 2457–2466 (2011)
7. Gasser, T.C., Ogden, R.W., Holzapfel, G.A.: Hyperelastic modelling of arterial layers with distributed collagen fibre orientations. J. R. Soc. Interface. **3**, 15–35 (2006)
8. Hayashi, K.: Experimental approaches on measuring the mechanical properties and constitutive laws of arterial walls. J. Biomech. Eng. **115**, 481488 (1993)
9. Holzapfel, G.A., Gasser, T.C., Ogden, R.W.: A new constitutive framework for arterial wall mechanics and a comparative study of material models. J. Elasticity **61**, 148 (2000)
10. Holzapfel, G.A., Ogden, R.W.: Constitutive modeling of arteries. Proc. Royal Society A **466**, 1551–1597 (2010)
11. Holzapfel, G.A., Sommer, G., Gasser, C.T., Regitnig, P.: Determination of the layer-specific mechanical properties of human coronary arteries with non-atherosclerotic intimal thickening, and related constitutive modelling. Am. J. Physiol. Heart Circ. Physiol. **289**, H2048–2058 (2005)
12. Humphrey, J.D.: An evaluation of pseudoelastic descriptors used in arterial mechanics. J. Biomech. Eng. **121**, 259–262 (1999)
13. Humphrey, J.D.: Cardiovascular Solid Mechanics: Cells, Tissues and Organs. Springer, Berlin (2001)
14. Humphrey, J.D.: Continuum biomechanics of soft biological tissues. Proc. R. Soc. Lond. A **459**, 1–44 (2003)
15. Lanir, Y.: Constitutive equations for fibrous connective tissues. J. Biomech. **16**, 1–12 (1983)
16. Li, W.: Damage models for soft tissues. J. Med. Biol. Eng. **36**, 285–307 (2016)
17. Li, D., Robertson, A.M.: A structural multi-mechanism damage model for cerebral arterial tissue. J. Biomech. Eng. **131**, 101013 (2009)
18. Li, D., Robertson, A.M., Lin, G.Y., Lovell, M.: Finite element modeling of cerebral angioplasty using a structural multi-mechanism anisotropic damage model. Int. J. Numer. Meth. Eng. **92**, 457–474 (2012)
19. Luo, Y., Duprey, A., Avril, S., Lu, J.: Characteristics of thoracic aortic aneurysm rupture in vitro. Acta. Biomater. **42**, 286–295 (2016)
20. Maher, E., Creane, A., Lally, C., Kelly, D.J.: An anisotropic inelastic constitutive model to describe stress softening and permanent deformation in arterial tissue. J. Mech. Behav. Biomed. Mater. **12**, 9–19 (2012)
21. Marini, G., Maier, A., Reeps, C., Eckstein, H.H.: A continuum description of the damage process in the arterial wall of abdominal aortic aneurysms. Int. J. Numer. Meth. Biomed. Eng. **28**, 87–99 (2012)
22. Natali, A., Pavan, P., Carniel, E.L., Lucisano, M.E., Taglialavoro, G.: Anisotropic elasto-damage constitutive model for the biomechanical analysis of tendons. Med. Eng. Phys. **27**, 209–214 (2005)
23. Ogden, R.W.: Non-Linear Elastic Deformations. Dover (1997)
24. Ogden, R.W.: Anisotropy and nonlinear elasticity in arterial wall mechanics. In: Holzapfel, G.A., Ogden, R.W. (eds.) 2009 Biomechanical Modeling at the Molecular, Cellular and Tissue Levels. Springer (2009)
25. Polindara, C., Waffenschmidt, T., Menzel, A.: Simulation of balloon angioplasty in residually stressed blood vessels - application of a gradient-enhanced fibre damage model. J Biomech, in press (2016)
26. Pena, E., Doblare, M.: An anisotropic pseudo-elastic approach for modelling Mullins effect in fibrous biological materials. Mech. Res. Commun. **36**, 784–790 (2009)
27. Takamizawa, K., Hayashi, K.: Strain energy density function and uniform strain hypothesis for arterial mechanics. J. Biomech. **20**, 7–17 (1987)
28. Volokh, K.Y.: Hyperelasticity with softening for modeling materials failure. J. Mech. Phys. Solids **55**, 2237–2264 (2007)
29. Volokh, K.: Prediction of arterial failure based on a microstructural bi-layer fibermatrix model with softening. J. Biomech. **41**, 447–453 (2008)
30. Volokh, K.: Modeling failure of soft anisotropic materials with application to arteries. J. Mech. Behav. Biomed. Mater. **4**, 1582–1594 (2011)

31. Volokh, K.Y.: Review of the energy limiters approach to modeling failure of rubber. Rubber. Chem. Technol. **86**, 470–487 (2013)
32. Volokh, K.Y.: On irreversibility and dissipation in hyperelasticity with softening. J. Appl. Mech. **81**, 074501 (2014)
33. Volokh, K.Y.: Mechanics of Soft Materials. Springer, Berlin (2016)
34. Zulliger, M.A., Fridez, P., Hayashi, K., Stergiopulos, N.: A strain energy function for arteries accounting for wall composition and structure. J. Biomech. **37**, 989–1000 (2004)